arXiv:cond-mat/0301401v1 [cond-mat.str-el] 21 Jan 2003

Hole-Doping Effects on a Two-dimensional Kondo Insulator

Yasuhiro Saito, Akihisa Koga and Norio Kawakami

Department of Applied Physics, Osaka University, Suita, Osaka 565-0871, Japan

(Received February 2, 2008)

We study the effects of hole doping on the two-dimensional Heisenberg-Kondo model around the quantum critical point, where the spin liquid phase (Kondo insulator) and the magnetically ordered phase are separated via a second-order phase transition. By means of the self-consistent Born approximation within the bond operator formalism as well as the standard spin wave theory, we discuss dynamical properties of a doped hole. It is clarified that a quasi-particle state stabilized in the spin liquid phase is gradually obscured as the system approaches the quantum critical point. This is also the case for the magnetically ordered phase. We argue the similarity and the difference between these two cases.

KEYWORDS: Kondo Insulator, bond operator, spin wave, self-consistent Born approximation

1. Introduction

Heavy fermion systems realized in rare-earth compounds have attracted much interest over many years. They show a variety of striking phenomena due to strong electron correlations. In metallic systems, the electron mass is renormalized to a huge value by the *f*-*f* Coulomb interaction.[1)] Such renormalization effects are also relevant for the insulating phase, leading to the Kondo insulator possessing both of the spin and charge gaps renormalized by electron correlations.[2,3)] Since these metallic and insulating states have essentially the same origin of electron correlations, it is interesting to ask how the Kondo insulator is changed to the heavy fermion metallic system upon hole doping.

Another interesting aspect in heavy fermion systems is that some of unusual static and dynamical properties are related to the fact that the system is located in the vicinity of a quantum critical point.[4–14)] For instance, the anomalous non-Fermi-liquid temperature dependence in the specific heat and the susceptibility observed in rare-earth compounds such as $CeCu_{6-x}R_x$(R = Au, Ag),[15)] $CePd_2Si_2$,[16)] $CeNi_2Ge_2$,[17)] $U_{1-x}Y_xPd_3$,[18)] $Ce_xLa_{1-x}Ru_2Si_2$[19)] is caused by large quantum fluctuations reflecting the phase transition to the antiferromagnetically ordered phase. In this way, strong quantum fluctuations near the critical point[20)] give rise to rich and attractive phenomena in rare-earth systems.

Stimulated by these interesting topics, we consider a simplified model of the Kondo insulator, which possesses the quantum critical point between the Kondo insulating phase and the antiferromagnetic phase. To be precise, we employ the two-dimensional Heisenberg-Kondo model, for which the charge degree of freedom is frozen at half filling, and the remaining spin sector is either in the spin liquid phase or the antiferromagnetically ordered phase at zero temperature. We investigate the effects of hole doping on the model with particular emphasis on the hole dynamics near the quantum critical point. Although the effects of hole doping into the Kondo insulator have been addressed so far,[3)] we think that the dynamics of a doped hole has not been discussed in detail. Also, in some respects, the present investigation is closely related to those done for the two-dimensional Heisenberg model in connection with the high T_c superconductors.[21–24)]

This paper is organized as follows. In Sec. 2, we introduce the two-dimensional Heisenberg-Kondo model and summarize the basic properties of the model. In Sec. 3, we study the hole dynamics, when it is doped into the spin liquid phase, by combining the self-consistent Born approximation with the bond-operator formalism. Similar analysis is performed for the antiferromagnetic phase in Sec. 4 by exploiting the spin wave theory. A brief summary is given in Sec. 5.

2. Heisenberg-Kondo model

We investigate the two-dimensional Heisenberg-Kondo model having conduction electrons coupled to localized f-spins. The model is schematically drawn in Fig. 1. The Hamiltonian reads

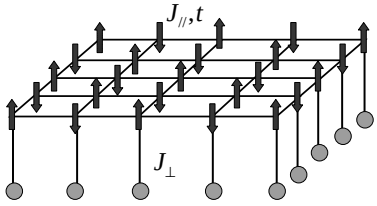

Fig. 1. Heisenberg-Kondo model on the square lattice. Spins of host electrons indicated by the arrows are antiferromagnetically coupled to localized f-spins indicated by the circles.

$$H = H_t + H_J, \tag{1}$$

$$H_J = J_{//} \sum_{<i,j>} \mathbf{S}_i^a \cdot \mathbf{S}_j^a + J_\perp \sum_i \mathbf{S}_i^a \cdot \mathbf{S}_i^b, \tag{2}$$

$$H_t = -t \sum_{<i,j>,\sigma} \hat{c}_{i,\sigma}^\dagger \hat{c}_{j,\sigma} + H.c., \tag{3}$$

with $\hat{c}_{i,\sigma} = [c_{i,\sigma}(1 - n_{i,-\sigma})]$, where $c_{i,\sigma}$ annihilates a conduction electron with spin $\sigma(=\uparrow,\downarrow)$ at the ith site. The corresponding spin operator is defined by $\mathbf{S}_i^a = \frac{1}{2}\sum_{\sigma,\sigma'} c_{i,\sigma}^\dagger \tau_{\sigma,\sigma'} c_{i,\sigma'}$, where τ is the Pauli matrix. The operator of an $s = 1/2$ f-spin is denoted by $\mathbf{S}_i^b$. The exchange couplings $J_{//}$ and $J_\perp$ are assumed to be antiferromagnetic. For convenience, we set hopping t as

unity and introduce the ratio $j = J_{//}/J_{\perp}$. At half filling, the system is in the spin-liquid insulating phase with both of the spin and charge gaps for smaller j, which may be a proper model of the Kondo insulator. We note that magnetic properties for $j = 0$ have already been discussed.[25–29] An interesting aspect in the model is that there exists a quantum phase transition at j_c (≈ 0.75, 8-th order series expansion)[30] from the spin-liquid phase (Kondo insulator) to the magnetically ordered phase as j increases. Therefore, the system realizes a quantum critical point at $j = j_c$, where the spin gap vanishes, but a long-range order still does not develop. This specific condition may give rise to anomalous behavior of a doped hole, reflecting large quantum fluctuations.

In order to discuss dynamical properties of a hole-doped Kondo insulator in the vicinity of the quantum critical point, we make use of either the bond-operator approach[31–33] or the spin wave approach. These methods are appropriate to discuss magnetic properties in the spin liquid phase and the magnetically ordered phase, respectively. We further exploit the self-consistent Born approximation(SCBA),[21–24,34] in which the motion of hole can be treated as a scattering problem in the host spin system. In the following, we separately discuss dynamical properties of a doped hole in the spin liquid phase and the magnetically ordered phase.

3. Hole doping in the spin-liquid phase

We begin with dynamical properties of a doped hole in the spin liquid phase (Kondo insulator) having the spin gap for excitations. For this purpose, we use the bond-operator representation, which is useful to deal with the spin-singlet state.

3.1 bond-operator representation

When the Kondo coupling between the host spins and localized spins is fairly strong, the dimer singlet is formed at each site, which may be a good starting point to describe the spin liquid phase. This condition allows us to introduce six kinds of the bond operators, which are defined at each site as,

$$\begin{aligned}
s_n^\dagger|0\rangle &= \frac{1}{\sqrt{2}}(|\uparrow\downarrow\rangle - |\downarrow\uparrow\rangle),\\
t_{x,n}^\dagger|0\rangle &= \frac{-1}{\sqrt{2}}(|\uparrow\uparrow\rangle - |\downarrow\downarrow\rangle),\\
t_{y,n}^\dagger|0\rangle &= \frac{i}{\sqrt{2}}(|\uparrow\uparrow\rangle + |\downarrow\downarrow\rangle),\\
t_{z,n}^\dagger|0\rangle &= \frac{1}{\sqrt{2}}(|\uparrow\downarrow\rangle + |\downarrow\uparrow\rangle),\\
a_{n,\uparrow}^\dagger|0\rangle &= |\circ\uparrow\rangle,\\
a_{n,\downarrow}^\dagger|0\rangle &= |\circ\downarrow\rangle, \qquad (4)
\end{aligned}$$

where ket states are specified by the configuration of a conduction electron and an f-electron [$\circ$ represents an unoccupied (hole) site]. Here, the operators $s^\dagger$ and $t_\alpha^\dagger(\alpha = x, y, z)$ obey the bosonic commutation relation, while the operator $a^\dagger$ the fermionic anticommutation relation. To restrict the physical states to either singlet, triplet or pseudofermion, the above operators are subjected to the constraint,

$$s_n^\dagger s_n + \sum_\alpha t_{\alpha,n}^\dagger t_{\alpha,n} + \sum_\sigma a_{n,\sigma}^\dagger a_{n,\sigma} = 1. \qquad (5)$$

In the spin liquid phase, the boson s is condensed, which results in the finite value of $< s_n >= \bar{s}$. Then the spin Hamiltonian H_J is diagonalized in the Fourier space as,

$$\begin{aligned}
H_J &= \sum_{\mathbf{k},\alpha} \omega_{\mathbf{k}} \gamma_{\alpha,\mathbf{k}}^\dagger \gamma_{\alpha,\mathbf{k}} + \text{const.}, \qquad (6)\\
\omega_{\mathbf{k}} &= J_\perp \sqrt{1 + 2e_{\mathbf{k}}},
\end{aligned}$$

where $e_{\mathbf{k}} = j\bar{s}^2 Q(\mathbf{k})$ with $Q(\mathbf{k}) = \frac{1}{2}(\cos k_x + \cos k_y)$. Here, we have introduced the normal-mode operator $\gamma_{\alpha,\mathbf{k}}^\dagger$ related to $t_{\alpha,\mathbf{k}}^\dagger$ via the Bogoliubov transformation,

$$t_{\alpha,\mathbf{k}}^\dagger = u_{\mathbf{k}} \gamma_{\alpha,\mathbf{k}}^\dagger + v_{\mathbf{k}} \gamma_{\alpha,-\mathbf{k}}, \qquad (7)$$

where $v_{\mathbf{k}}^2 = 1/2\{J_\perp(1 + e_{\mathbf{k}})/\omega_{\mathbf{k}} - 1\}$, $u_{\mathbf{k}}^2 = 1/2\{J_\perp(1 + e_{\mathbf{k}})/\omega_{\mathbf{k}} + 1\}$.

When a hole is doped into the system, the condensate density of the singlet is determined by the hard-core constraint eq. (5) as

$$\bar{s} = 1 - \frac{3}{N}\sum_{\mathbf{q}} v_{\mathbf{q}}^2. \qquad (8)$$

In the bond-operator representation, the operator for a physical electron is written by two bond operators as,

$$\begin{aligned}
\hat{c}_{n,\sigma} = \frac{1}{\sqrt{2}} \quad & [\quad a_{n,\bar{\sigma}}^\dagger (p_\sigma s_n + t_{z,n})\\
& + \quad a_{n,\sigma}^\dagger (p_{\bar{\sigma}} t_{x,n} + i t_{y,n})], \qquad (9)
\end{aligned}$$

where $p_\sigma = +(-)$, $\bar{\sigma} = \downarrow (\uparrow)$ for $\sigma = \uparrow (\downarrow)$. We thus obtain the Hamiltonian for electron hopping,

$$\begin{aligned}
H_t &= \frac{t}{2}\bar{s}^2 \sum_{<i,j>,\sigma} a_{i,\sigma}^\dagger a_{j,\sigma} - t\bar{s} \sum_{<i,j>} (\mathbf{t}_j^\dagger \mathbf{T}_{i,j} + \mathbf{t}_i^\dagger \mathbf{T}_{j,i})\\
&+ \frac{t}{2} \sum_{<i,j>,\sigma} \mathbf{t}_i^\dagger \mathbf{t}_j a_{j,\sigma}^\dagger a_{i,\sigma} - t \sum_{<i,j>} i(\mathbf{t}_i^\dagger \times \mathbf{t}_j)\mathbf{T}_{j,i}\\
&+ H.c. \qquad (10)
\end{aligned}$$

with $\mathbf{t}_i^\dagger = (t_{x,i}^\dagger, t_{y,i}^\dagger, t_{z,i}^\dagger)$ and

$$\mathbf{T}_{m,n} = \frac{1}{2}\sum_{\sigma_1,\sigma_2} a_{m,\sigma_1}^\dagger \tau_{\sigma_1,\sigma_2} a_{n,\sigma_2}, \qquad (11)$$

where $(\mathbf{T}_{m,n})^\dagger = \mathbf{T}_{n,m}$. This Hamiltonian is spin rotationally invariant, reflecting the fact that the system has no magnetic order.

3.2 Green function

To discuss the dynamics of a doped hole, we define the retarded Green functions for a pseudofermion and a

physical electron as

$$G_\sigma(\mathbf{k},t) = -i\Theta(t) < D|\{a_{\mathbf{k},\sigma}(t), a^\dagger_{\mathbf{k},\sigma}\}|D >, \quad (12)$$

$$G^c_\sigma(\mathbf{k},t) = -i\Theta(t) < D|\{\hat{c}_{\mathbf{k},\sigma}(t), \hat{c}^\dagger_{\mathbf{k},\sigma}\}|D >, \quad (13)$$

where $|D>$ represents the spin-singlet ground state. For small j, renormalization effects due to the two triplet vertices in eq. (10) are of minor importance, so that we will discard them in the following. We then arrive at the Hamiltonian for a doped hole as

$$H_0 = 2t\bar{s}^2 \sum_{\mathbf{k}} Q(\mathbf{k}) a^\dagger_{\mathbf{k},\sigma} a_{\mathbf{k},\sigma}, \quad (14)$$

$$V = -\frac{1}{\sqrt{N}} \sum_{\mathbf{k},\mathbf{q},\sigma_1,\sigma_2} \{M_{\mathbf{kq}} \gamma^\dagger_{\mathbf{q}} a^\dagger_{\mathbf{k}-\mathbf{q},\sigma_1} \tau_{\sigma_1,\sigma_2} a_{\mathbf{k},\sigma_2} + M_{\mathbf{kq}} \gamma_{-\mathbf{q}} a^\dagger_{\mathbf{k}-\mathbf{q},\sigma_1} \tau_{\sigma_1,\sigma_2} a_{\mathbf{k},\sigma_2}\}, \quad (15)$$

where the element M in the perturbation term V represents the scattering of a triplet boson,

$$M_{\mathbf{kq}} = t\bar{s}\{Q(\mathbf{k}) + Q(\mathbf{k}-\mathbf{q})\}(u_{\mathbf{q}} + v_{\mathbf{q}}). \quad (16)$$

We wish to note that the SCBA is useful to deal with the Hamiltonian eqs. (14) and (15). In terms of the bare Green functions for a pseudofermion and a triplet-boson,

$$G^0_\sigma(\mathbf{k},\omega) = \frac{1}{\omega - 2t\bar{s}^2 Q(\mathbf{k})}, \quad (17)$$

$$D_\alpha(\mathbf{k},\omega) = \frac{1}{\omega - \omega_{\mathbf{k}}}, \quad (18)$$

we can evaluate the self-energy of a pseudofermion in the SCBA, which is diagramatically shown in Fig. 2. The

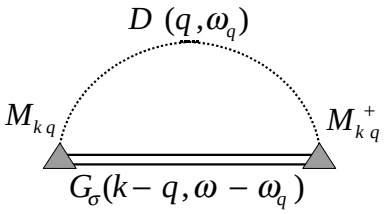

Fig. 2. Self-energy of a pseudofermion in the SCBA. The triangle represents the scattering matrix of a triplet boson.

Green function defined by $G_\sigma(\mathbf{k},\omega) = [G^0_\sigma(\mathbf{k},\omega)^{-1} - \Sigma_\sigma(\mathbf{k},\omega)]^{-1}$ is determined via the self-consistent equation,

$$\mathbf{\Sigma}_\sigma(\mathbf{k},\omega) = \frac{3}{N}\sum_{\mathbf{q}} M^2_{\mathbf{kq}} [G^0_\sigma(\mathbf{k}-\mathbf{q},\omega-\omega_q)^{-1} - \mathbf{\Sigma}_\sigma(\mathbf{k}-\mathbf{q},\omega-\omega_{\mathbf{q}})]^{-1}, \quad (19)$$

where $\omega = \omega + i\eta$ with $\eta \to 0^+$.

To obtain the physical Green function of an electron, we introduce the elements as

$$\alpha_{\mathbf{k},\sigma} = s\langle D|a_{\mathbf{k},\bar{\sigma}}\hat{c}_{\mathbf{k},\sigma}|D\rangle = \frac{\pm s}{\sqrt{2}},$$

$$\beta_{\mathbf{kq},\sigma} = \langle D|(\gamma_{\mathbf{q}} a_{\mathbf{k}-\mathbf{q}})_{(1/2)(\mp 1/2)}\hat{c}_{\mathbf{k},\sigma}|D\rangle = \pm\sqrt{\frac{3}{2N}} v_q, \quad (20)$$

which relate the Green function of a pseudofermion to that of a real electron. When $j < j_c$, the density of triplets is small in the ground state, i.e., $0 < v_{\mathbf{q}} \ll 1$. Then it is legitimate to use a perturbative evaluation of two-particle propagator within the random-phase approximation (RPA).[34] This gives us the Green function,

$$\begin{aligned} G^c_\sigma(k,\omega) &= \alpha_{k,\sigma} G_\sigma(k,\omega)\alpha_{k,\sigma} \\ &+ \sum_q \beta_{kq,\sigma} G_\sigma(k-q,\omega-\omega_q)\beta_{kq,\sigma} \\ &+ \left(\alpha_{k,\sigma} G_\sigma(k,\omega), \sqrt{\frac{3}{N}}\sum_q \beta_{kq,\sigma} G_\sigma(k-q,\omega-\omega_q) M^\dagger_{kq}\right) \\ &\times \begin{pmatrix} 1 & -\frac{3}{N}\sum_q M_{kq} G_\sigma(k-q,\omega-\omega_q) M^\dagger_{kq} \\ -G_\sigma(k,\omega) & 1 \end{pmatrix}^{-1} \\ &\times \begin{pmatrix} \sqrt{\frac{3}{N}}\sum_q M_{kq} G_\sigma(k-q,\omega-\omega_q)\beta_{kq,\sigma} \\ G_\sigma(k,\omega)\alpha_{k,\sigma} \end{pmatrix}. \end{aligned} \quad (21)$$

This completes the formulation of the SCBA for a hole doped in the spin liquid phase.

3.3 numerical results

Before discussing the nature of the hole-propagator, we check how well our bond-operator approach works at half filling. In Fig. 3, we show the spin-triplet excitation gap calculated by several different methods. The

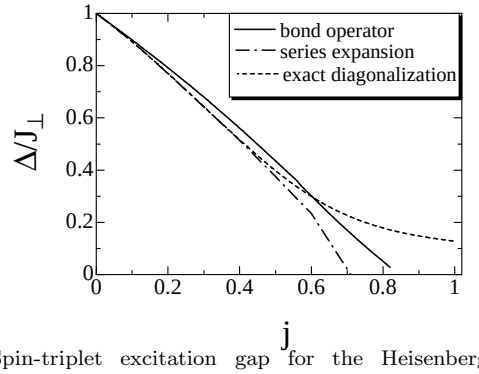

Fig. 3. Spin-triplet excitation gap for the Heisenberg-Kondo model at half filing. The solid, dash-dotted, and broken lines represent the spin gap computed by the bond-operator method, the series expansion method (9-th order), and the exact diagonalization (3×4 system).

phase transition point was evaluated approximately as $j_c \simeq 0.75$,[30] so that we can say that the bond-operator approach may describe the spin-liquid phase rather well in a wide range of the parameters.

Let us now turn to the hole-doped case. From now on, we set $\eta = 0.1$. Shown in Fig. 4 is the spectral function of a doped hole computed by the SCBA. When $J_\perp = 5$ and $j = 0.5$, we find a dominant dispersive peak in the spectral function, which originates from the first term in the Hamiltonian (10), indicating the coherent motion of a doped hole without triplet excitations. Namely, the low-energy edge of the spectrum determined by the poles of the Green function on the real axis remains separated by gap from the continuum of multimagnon shake off. The corresponding dispersion of a quasiparticle is given

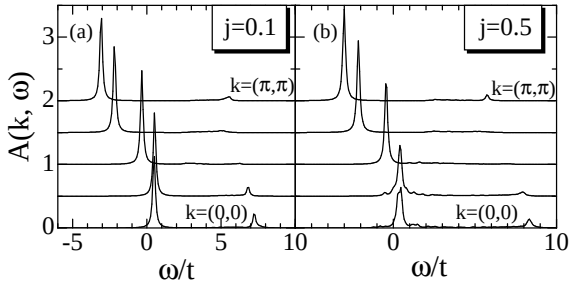

Fig. 4. Spectral function of a doped hole in the spin liquid phase for $J_\perp = 5$, $j = 0.1$ (a) and $j = 0.5$ (b). The momentum of each spectral function is chosen as $\mathbf{k} = (0,0), (\pi/4,\pi/4), (\pi/2,\pi/2), (3\pi/4,3\pi/4), (\pi,\pi)$ from the bottom to the top.

by

$$\epsilon_{\mathbf{k}} = 2t\bar{s}^2 Q(\mathbf{k}) - \frac{3}{N}\sum_{\mathbf{q}} \frac{M^2_{\mathbf{kq}}}{\omega_{\mathbf{q}}}. \tag{22}$$

Shown in Fig. 5 is the quasi-particle dispersion thus ob-

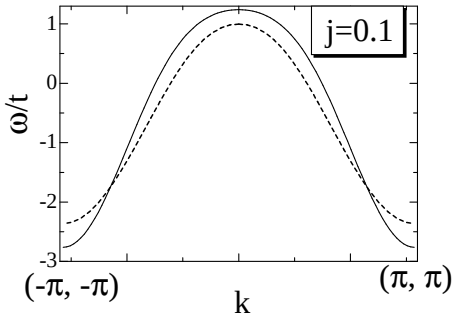

Fig. 5. Dispersion relation of a doped hole for $J_\perp = 5$ and $j = 0.1$. The solid (broken) line is obtained by the SCBA (series expansion of the 7th order).

tained. The comparison of this with the spectral function in Fig. 4 confirms that the sharp peak is indeed developed along the dispersion curve. This implies that the quasi-particle state is quite stable in this parameter region. We also calculate the dispersion of a hole by means of the series expansion,[35] in which the excitation energy is expanded in j and t up to the seventh order. The results are shown in Fig. 5 by the broken line. We find that the results obtained by the SCBA are consistent with those obtained by the series expansion. Increasing the interdimer coupling $J_{//}$, antiferromagnetic correlations are gradually enhanced and the spin gap is decreased. Then a doped hole suffers from the scattering by low-lying spin excitations, making the peak structure on the dispersion curve somehow broadened. This tendency is clearly observed in the peak around $\mathbf{k} = (0,0)$ in Fig. 4(b). When $J_\perp = 1$ and $j = 0.5$, the spin gap becomes small. In this case, the quasiparticle peak around $\mathbf{k} = (0,0)$ is completely smeared, as shown in Fig. 6. The large portion of the corresponding weight is shifted to the incoherent parts in higher energy region. The dispersion relation obtained approximately possesses a dip structure around the origin, as seen in Fig. 6(b). However, this structure may not be sensible, since the quasi-particle picture does not hold in this momentum

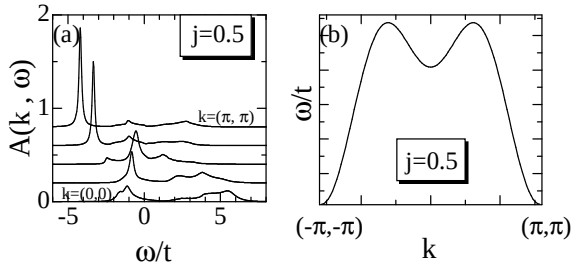

Fig. 6. Spectral function of a doped hole (a) and the corresponding dispersion relation (b) for $J_\perp = 1$ and $j = 0.5$. The momenta are chosen as in Fig. 4.

region. We note that even in this case, the spectrum around $\mathbf{k} = (\pi,\pi)$ still forms a rather sharp structure, implying that the hole motion with this momentum is not affected so much by spin excitations. For reference we show the width W of the quasi-particle band and the renormalization factor Z of the $\mathbf{k} = (0,0)$ state in Fig. 7. The latter quantity is defined by

$$Z(\mathbf{k}) = \left(1 - \frac{\partial \Sigma(\mathbf{k},\omega)}{\partial \omega}\right)^{-1}|_{\omega=\epsilon_{\mathbf{k}}}, \tag{23}$$

which corresponds to the weight of the quasi-particle state. It is seen that the band width becomes small as the system approaches the quantum critical point. At the same time, the weight of the quasi-particle decreases monotonically near the critical point, being consistent with the disappearance of the well-defined quasi-particle state. We have so far discussed spectral properties of a

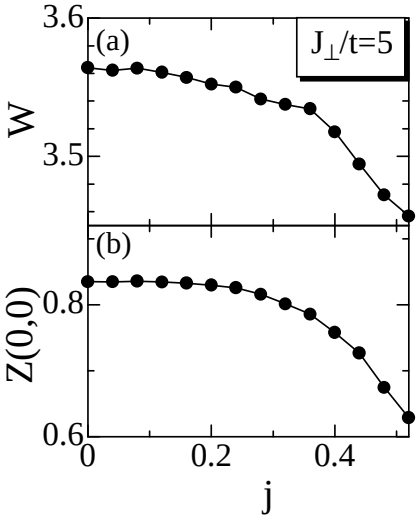

Fig. 7. Plots of the width W of the quasi-particle band and the renormalization factor Z for the spin-liquid phase.

doped hole in the spin liquid phase, and shown that well-defined quasi-particle states in the $j \ll j_c$ are gradually obscured when the system approaches the quantum critical point $j = j_c$. In particular, the spectrum around $\mathbf{k} = (0,0)$ is affected considerably. It is to be noted here that these characteristic properties may not be specific to the present model, but more generically hold for hole-doped systems in the spin liquid phase.

Before closing the section, we wish to make closer com-

parison of the present SCBA with the exact diagonalization calculation by taking the one-dimensional model. In Fig. 8, we show the spectral function and the dispersion relation for the one-dimensional Heisenberg-Kondo model. It is found that the results of the SCBA agree

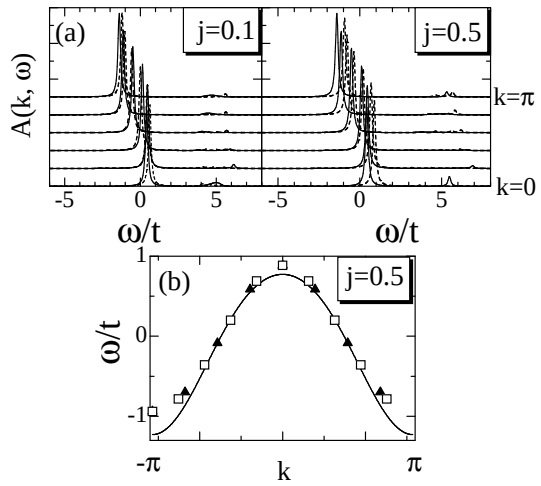

Fig. 8. (a): Spectral function of a doped hole in the one-dimensional Kondo insulator at $J_\perp = 5$. The solid line is obtained by the SCBA and the dashed line by the exact diagonalization for the system of 10 sites. The momentum is varied as $k = 0, \pi/4, \pi/2, 3\pi/4, \pi$. (b): The solid line is the dispersion relation obtained by the SCBA at $J_\perp = 5$. The triangles and the squares represent the results obtained by the exact diagonalization for the system of 8 and 10 sites, respectively.

fairly well with those of the exact diagonalization, both of which show the well-defined quasi-particle state. In this way, even in one dimension, the existence of the spin gap plays an important role in stabilizing the quasi-particle state in the spin liquid phase.

4. Hole doping in the antiferromagnetic phase

We next discuss the effects of hole doping on the antiferromagnetically ordered phase $j > j_c$. In this case, excitations in the host spin system may be well described by the spin wave theory, which we will use in the following discussions.

4.1 spin-wave theory

We exploit the Holstein-Primakoff transformation, which expresses the spin-1/2 operators $\mathbf{S}_i^a$ and $\mathbf{S}_i^b$ in terms of the Bose operators b and d as,

$$\begin{aligned} S_i^{a,+} &= \sqrt{(1-b_i^\dagger b_i)}b_i \\ S_i^{a,-} &= b_i^\dagger\sqrt{(1-b_i^\dagger b_i)} \\ S_i^{a,z} &= \frac{1}{2} - b_i^\dagger b_i \\ S_i^{b,+} &= d_i^\dagger\sqrt{(1-d_i^\dagger d_i)} \\ S_i^{b,-} &= \sqrt{(1-d_i^\dagger d_i)}d_i \\ S_i^{b,z} &= -\frac{1}{2} + d_i^\dagger d_i \end{aligned} \qquad (24)$$

for each sublattice. By performing the Fourier transformation and then applying the standard Bogoliubov transformation, the Hamiltonian H_J for the spin sector can be diagonalized as

$$H_J = \sum_{\mathbf{k}} (\omega_{1\mathbf{k}}\alpha_{\mathbf{k}}^\dagger\alpha_{\mathbf{k}} + \omega_{2\mathbf{k}}\beta_{\mathbf{k}}^\dagger\beta_{\mathbf{k}}) + \text{const.}, \qquad (25)$$

with $\omega_{1\mathbf{k}} = 4J_{//}\sqrt{B_{\mathbf{k}} - A_{\mathbf{k}}}$ and $\omega_{2\mathbf{k}} = 4J_{//}\sqrt{B_{\mathbf{k}} + A_{\mathbf{k}}}$, where $A_{\mathbf{k}} = 1/16[4 + 4j^{-1} + Q(\mathbf{k})^2(j^{-2} - 4j^{-1} - 8) + 4Q(\mathbf{k})^4]^{1/2}$, $B_{\mathbf{k}} = 1/8(1 - Q(\mathbf{k})^2 + j^{-1}/2)$. Here, we have ignored the hard-core constraint in eq. (24) since it has little effect on low-energy properties for small values of j^{-1}. The Bogoliubov transformation from the original bosons $(b_{\mathbf{k}}, d_{\mathbf{k}})$ to the normal-mode bosons $(\alpha_{\mathbf{k}}, \beta_{\mathbf{k}})$ takes the form,

$$\begin{pmatrix} b_{\mathbf{k}} \\ d_{\mathbf{k}} \\ b_{-\mathbf{k}}^\dagger \\ d_{-\mathbf{k}}^\dagger \end{pmatrix} = \begin{pmatrix} \Gamma_{\mathbf{k}} & -\Theta_{\mathbf{k}} \\ -\Theta_{\mathbf{k}} & \Gamma_{\mathbf{k}} \end{pmatrix} \begin{pmatrix} \alpha_{\mathbf{k}} \\ \beta_{\mathbf{k}} \\ \alpha_{-\mathbf{k}}^\dagger \\ \beta_{-\mathbf{k}}^\dagger \end{pmatrix}, \qquad (26)$$

where

$$\begin{aligned} \Gamma_{\mathbf{k}} &= \begin{pmatrix} R_{\mathbf{k},+} & R_{\mathbf{k},-} \\ I_{\mathbf{k},+} & I_{\mathbf{k},-} \end{pmatrix} \\ \Theta_{\mathbf{k}} &= \begin{pmatrix} L_{\mathbf{k},+} & L_{\mathbf{k},-} \\ 1 & 1 \end{pmatrix} \end{aligned} \qquad (27)$$

and

$$\begin{aligned} R_{\mathbf{k},\pm} &= \frac{8E_{\mathbf{k},\pm}}{j^{-1}p_{\mathbf{k},\pm}} \\ I_{\mathbf{k},\pm} &= \frac{2}{Q(\mathbf{k})F_{\mathbf{k},\pm}}\{-\frac{j^{-2}}{64} + E_{\mathbf{k},\pm}(\frac{1}{2} + F_{\mathbf{k},\pm})\}/p_{\mathbf{k},\pm} \\ L_{\mathbf{k},\pm} &= \frac{1}{Q(\mathbf{k})j^{-1}}[16\{-\frac{j^{-2}}{64} + E_{\mathbf{k},\pm}(\frac{1}{2} + F_{\mathbf{k},\pm})\}]/p_{\mathbf{k},\pm} \end{aligned} \qquad (28)$$

with $p_{\mathbf{k},\pm}^2 = R_{\mathbf{k},\pm}^2 + I_{\mathbf{k},\pm}^2 - L_{\mathbf{k},\pm}^2 - 1$. Here, $E_{\mathbf{k},\pm} = j^{-1}/8 + \sqrt{B_{\mathbf{k}} \mp A_{\mathbf{k}}}$, $F_{\mathbf{k},\pm} = j^{-1}/8 - \sqrt{B_{\mathbf{k}} \mp A_{\mathbf{k}}}$.

We show the dispersion relation obtained for the undoped case in Fig. 9, in which gapless excitations in

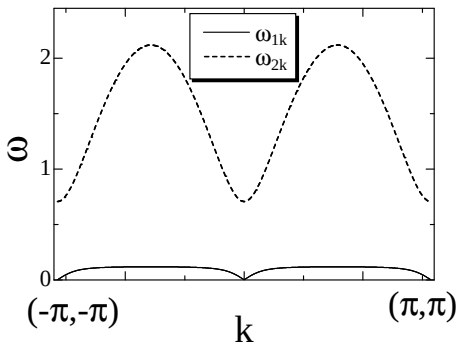

Fig. 9. Spin wave spectra at $J_{//} = 1, j^{-1} = 0.25$ along the line in the momentum space from $\mathbf{k} = (-\pi, -\pi)$ to $\mathbf{k} = (\pi, \pi)$. The solid line indicates $\omega_{1\mathbf{k}}$ and the dashed line $\omega_{2\mathbf{k}}$.

the low-energy region ω_1 and gapful excitations with a large dispersion ω_2 appear. It is easily seen that ω_1 is mainly contributed by localized spins, while ω_2 by conduction electrons in this parameter region. To discuss

the stability of the magnetically ordered ground state, we calculate the spin deviation ΔS_1 for f-spins and ΔS_2 for conduction electrons,

$$\Delta S_1 =< d^\dagger_{\mathbf{k}} d_{\mathbf{k}} >= \frac{1}{N}\sum_{\mathbf{k}}(p^2_{\mathbf{k},+} + p^2_{\mathbf{k},-}),$$

$$\Delta S_2 =< b^\dagger_{\mathbf{k}} b_{\mathbf{k}} >= \frac{1}{N}\sum_{\mathbf{k}}(L^2_{\mathbf{k},+} + L^2_{\mathbf{k},-}). \tag{29}$$

In Fig. 10, we show the staggered magnetization $S-\Delta S$ as a function of j^{-1}. When $J_\perp = 0$ ($j^{-1} = 0$), the

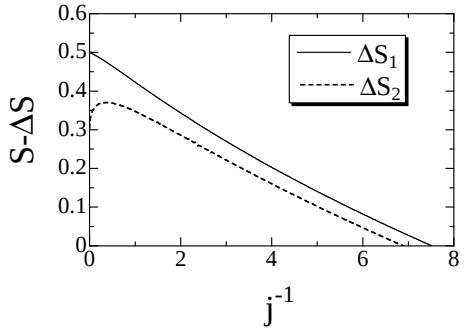

Fig. 10. Staggered magnetizations $S-\Delta S_1$ (solid line) and $S-\Delta S_2$ (dashed line) as a function of j^{-1}.

system is reduced to the Heisenberg antiferromagnet on the square lattice,[36] which is completely separated from free f-spins S^b. The introduction of the exchange coupling $J_\perp$ enhances spin correlations between conduction electrons and localized spins. Then the magnetization of conduction electrons once increases and has a maximum value around $j^{-1} \approx 0.37$. Further increase of the exchange coupling enhances the dimer correlation, and thereby suppresses the magnetization. Note that the ordered state is stabilized up to the critical value $j_c^{-1} \approx 6.97$ for conduction electrons, but $j_c^{-1} \approx 7.60$ for localized spins. This pathological result means that beyond $j_c^{-1} \approx 6.97$ our spin-wave theory may break down. Since the critical value $j_c^{-1} \approx 6.97$ is slightly larger than that obtained by the series expansion, we believe that our spin wave theory can properly describe the ordered state except for the region very close to the phase transition point.

4.2 Green function

Let us now turn to the hole-doped case. In the spin-wave approximation, the Hamiltonian for electron hopping reads

$$H_t = -t\sum_{<i,j>}\{h^\dagger_i h_j[b^\dagger_j(1-b^\dagger_i b_i) + (1-b^\dagger_j b_j)b_i] + H.c.\}, \tag{30}$$

where $h_i(= c^\dagger_{i\sigma})$ is the annihilation operator of a hole. This is rewritten in terms of the normal modes as,

$$H_t = -\frac{4t}{\sqrt{N}}\sum_{\mathbf{k},\mathbf{q}} h^\dagger_{\mathbf{k}} h_{\mathbf{k}-\mathbf{q}}[(R_{\mathbf{q},+}\gamma_{\mathbf{k}-\mathbf{q}} - L_{\mathbf{q},+}\gamma_{\mathbf{k}})(\alpha_{\mathbf{q}} + \alpha^\dagger_{-\mathbf{q}}) + (R_{\mathbf{q},-}\gamma_{\mathbf{k}-\mathbf{q}} - L_{\mathbf{q},-}\gamma_{\mathbf{k}})(\beta_{\mathbf{q}} + \beta^\dagger_{-\mathbf{q}})]. \tag{31}$$

We introduce the following Green function of a doped hole,

$$G(\mathbf{k},t) = -i\langle\psi|T[h_{\mathbf{k}}(t)h^\dagger_{\mathbf{k}}(0)]|\psi\rangle, \tag{32}$$

where $|\psi\rangle$ is the ground state of the model and T is a time-ordering operator. When a doped hole hops in the lattice, the ordered state is perturbed and magnons are excited. Note that the motion of a hole scatters two types of magnons specified by $\alpha_{\mathbf{k}}$ and $\beta_{\mathbf{k}}$. By exploiting the SCBA for magnon scattering, we have the self-energy of the hole Green function as

$$\Sigma(\mathbf{k},\omega) = \Sigma^{(1)}(\mathbf{k},\omega) + \Sigma^{(2)}(\mathbf{k},\omega) \tag{33}$$

$$\Sigma^{(1)}(\mathbf{k},\omega) = \frac{16t^2}{N}\sum_{\mathbf{q}}(R_{\mathbf{q},+}\gamma_{\mathbf{k}-\mathbf{q}} - L_{\mathbf{q},+}\gamma_{\mathbf{k}})^2 G(\mathbf{k}-\mathbf{q},\omega-\omega_{1,\mathbf{q}})$$

$$\Sigma^{(2)}(\mathbf{k},\omega) = \frac{16t^2}{N}\sum_{\mathbf{q}}(R_{\mathbf{q},-}\gamma_{\mathbf{k}-\mathbf{q}} - L_{\mathbf{q},-}\gamma_{\mathbf{k}})^2 G(\mathbf{k}-\mathbf{q},\omega-\omega_{2,\mathbf{q}}). \tag{34}$$

When $J_{//} \gg J_\perp$ and t, one obtains the dispersion relation of a hole analytically as,

$$\epsilon_{\mathbf{k}} = -\xi_{1\mathbf{k}} - \xi_{2\mathbf{k}}$$

$$\xi_{1\mathbf{k}} = \frac{16t^2}{N}\sum_{\mathbf{q}}\frac{(R_{\mathbf{q},+}\gamma_{\mathbf{k}-\mathbf{q}} - L_{\mathbf{q},+}\gamma_{\mathbf{k}})^2}{\omega_{1\mathbf{q}}}$$

$$\xi_{2\mathbf{k}} = \frac{16t^2}{N}\sum_{\mathbf{q}}\frac{(R_{\mathbf{q},-}\gamma_{\mathbf{k}-\mathbf{q}} - L_{\mathbf{q},-}\gamma_{\mathbf{k}})^2}{\omega_{2\mathbf{q}}}. \tag{35}$$

4.3 numerical results

We show the spectral function in Fig. 11(a). When a

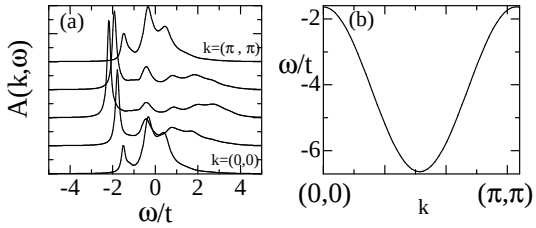

Fig. 11. (a) Spectral function of a doped hole. The momenta are chosen as in Fig. 4. (b) Dispersion relation given by Eq. (35): $j = 0.5$, $J_\perp = 10^{-5}$.

hole is doped into the system, the peak structure develops along the dispersion curve shown in Fig. 11(b), being consistent with those discussed in the doped Heisenberg antiferromagnet on the square lattice.[21–24] In particular, the peak is rather sharp in the low-energy region near $\mathbf{k} \approx (\pi/2, \pi/2)$. These results imply that the quasiparticle state defined by eq. (35) is stable in this parameter region.

Shown in Fig. 12 is the spectral function $A(\mathbf{k},\omega)$ when the exchange coupling $J_\perp$ is varied. For $j^{-1} = 0.25$, the quasi-particle state is well defined, which has a visible dispersion in the spectral function. When the exchange coupling $J_\perp$ increases, the quasiparticle state becomes less dispersive. Such flattening effect is more clearly seen in direct plots of the dispersion relation shown in Fig. 11.

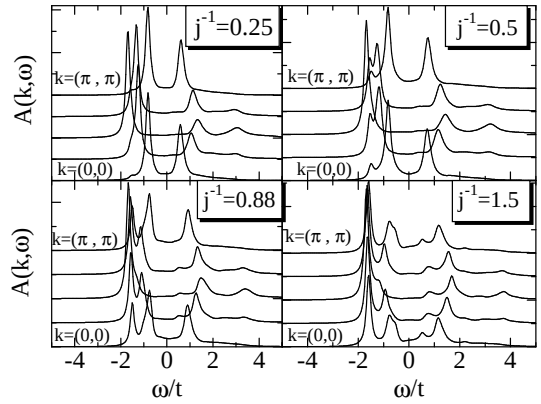

Fig. 12. Spectral function of a doped hole as a function of ω for $J_{//}$=0.8. The momenta are chosen as in Fig. 4.

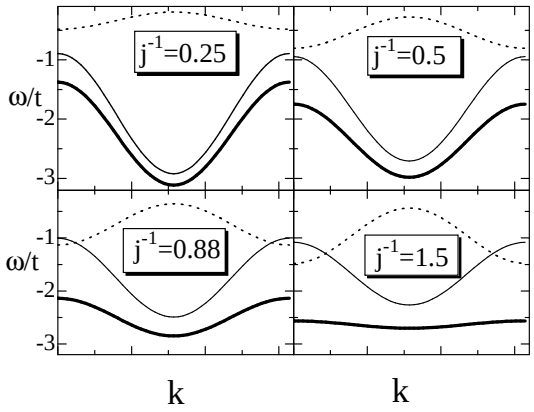

Fig. 13. Dispersion relation (bold line) of a doped hole in the antiferromagnetic phase for $J_{//} = 0.8$. Thin and broken lines represent the contributions from $\xi_{1\mathbf{k}}$ and $\xi_{2\mathbf{k}}$ in eq.(35).

13. The dispersive band for smaller $J_\perp$ is mainly contributed by conduction electrons. On the other hand, for larger $J_\perp$, conduction electrons and f-electrons are mixed up, which in turn gives rise to the flat dispersion near the critical point. In this region, other peaks with large weight appear besides the quasiparticle peak in the spectral function, as seen in Fig. 12. This implies that the quasiparticle picture does not hold anymore.

In Fig. 14 we show the width of the quasi-particle band and the renormalization factor. It is seen that both of these quantities become small as the system approaches the critical point, similarly to the case of the spin liquid phase discussed in the previous section. However, in closer comparison of these two cases, we see that the quasi-particle is less stable in the ordered phase, because the quasi-particle state in this case is dressed by gapless magnon excitations, making it somewhat difficult to distinguish the quasi-particle state from low-energy excited continuum.

5. Summary

We have investigated dynamical properties of a single hole doped into the Heisenberg-Kondo model on the square lattice. At half filling, the model is either in the disordered spin-liquid phase or the antiferromagnetically

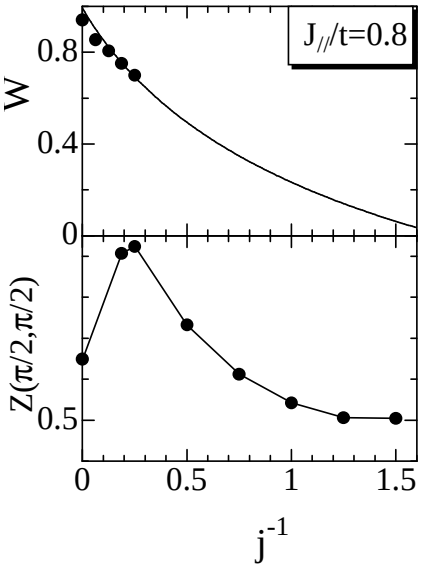

Fig. 14. Band width W for the quasi-particle and renormalization factor Z in the ordered phase. We show Z with $\mathbf{k} = (\pi/2, \pi/2)$, since this state has a rather clear peak structure. Solid circles are the results for the 8×8 system. The solid line for the width is computed from the analytic expression eq.(35). It is not easy to extract the correct values of W from the spectral function computed for larger $J_\perp$, so that we have plotted them only for the small $J_\perp$ region. The non-monotonic behavior in Z reflects a singular property of the limit $J_\perp \to 0$.

ordered phase. In the spin liquid phase, by employing the bond-operator representation, we have shown that a doped hole has the nature of a well-defined quasi-particle with the unambiguous dispersion relation. In the vicinity of the quantum critical point, however, the quasi-particle state is obscured due to the decrease of the spin gap. This effect appears most prominently in the region around $\mathbf{k} = (0, 0)$. Even in this case, it has shown that the spectrum around $\mathbf{k} = (\pi, \pi)$ still forms a sharp peak structure. In the antiferromagnetically ordered phase, we have encountered similar quasi-particle behavior of a doped hole, as in the spin-liquid phase. Namely, the quasi-particle state is smeared and its dispersion becomes flat as the system approaches the quantum critical point.

Although apparent properties are quite analogous in these two cases, there is the essential difference between them for the origin of the quasi-particle state: the quasi-particle in the spin liquid phase is stabilized in the presence of the spin gap, while that in the ordered phase is dressed by low-energy magnon excitations. We have indeed seen that this causes the difference in the stability of the quasi-particle state around the critical point.

In this paper, we have discussed the hole-doping effects by starting from two extreme limits. In these approaches, it is not easy to deal with the properties precisely just at the critical point. It is thus desirable to directly investigate anomalous properties such as the temperature dependence of the susceptibility around the critical regime. Also, it remains an interesting open problem what kind of unusual properties are expected when the finite density of holes are doped into the system around the critical point, which is now under consideration.

Acknowledgments

This work was partly supported by a Grant-in-Aid from the Ministry of Education, Science, Sports and Culture of Japan. A part of computations was done at the Supercomputer Center at Institute for Solid Physics, University of Tokyo and Yukawa Institute Computer Facility.

1) A. C. Hewson: The Kondo Problem to Heavy Fermions (Cambridge Univ. Press, Cambridge 1993).
2) S. Doniach, Physica B+C **91B**, 231 (1977).
3) See for a review, H. Tsunetsugu, M. Sigrist and K. Ueda, Rev. Mod. Phys. **69**, 809 (1997).
4) Y. Kuramoto and K. Miyake, J. Phys. Soc. Jpn. **59**, 2831 (1990).
5) B. Andraka and A. M. Tsvelik, Phys. Rev. Lett. **67**, 2886 (1991).
6) J. A. Hertz, Phys. Rev. B **14**, 1165 (1976).
7) A. J. Millis, Phys. Rev. B **48**, 7183 (1993).
8) T. Moriya and T. Takimoto, J. Phys. Soc. Jpn. **64**, 960 (1995).
9) M. A. Continentino, Phys. Rev. B **47**, 11587 (1993).
10) P. Schlottmann, Phys. Rev. B **59**, 12379 (1999).
11) P. Coleman, Physica B **259-261**, 353 (1999).
12) Q. Si, J. L. Smith, and K. Ingersent, Int. J. Mod. Phys. B **13**, 2331 (1999).
13) A. Rosch, Phys. Rev. Lett. **82**, 4280 (1999).
14) M. Lavagna and C. Pepin, Phys. Rev. B **62**, 6450 (2000).
15) H. von Lohneysen, A. Schroöder, M. Sieck and T. Trappmann, Phys. Rev. Lett. **72**, 3262 (1994).
16) N. D. Mathur, F. M. Grosche, S. R. Julian, I. R. Walker, D. M. Freye, R. K. W. Haselwimmer and G. G. Lonzarich, Nature **394**, 39 (1998).
17) F. Steglich, B. Buschinger, P. Gegenwart, M. Lohmann, R Helfrich, C. Langhammer, P. Hellmann, L. Donnevert, S. Thomas, A. Link, C. Geibel, M. Lang, G. Sparn and W. Assmus, J. Phys. Condens. Matter **8**, 9909 (1996).
18) C. L. Seaman, M. B. Maple, B. W. Lee, S. Ghamaty, M. S. Torikachvili, J.-S. Kang, L. Z. Liu, J. W. Allen, and D. L. Cox, Phys. Rev. Lett. **67**, 2882 (1991).
19) S. Kambe, S. Raymond, L.-P. Regnault, J. Flouquet, P. Lejay and P. Haen, J. Phys. Soc. Jpn. **65**, 3294 (1996).
20) S. Chakravarty, B. I. Halperin and D. R. Nelson, Phys. Rev. Lett. **60**, 1057 (1988).
21) S. Schmitt-Rink , C. M. Varma and A. E. Ruckenstein, Phys. Rev. Lett. **60**, 2793 (1988).
22) G. Martinez and P. Horsh, Phys. Rev. B **44**, 317 (1991).
23) Z. Liu and E. Manousakis, Phys. Rev. B **45**, 2425 (1992).
24) F. Magsiglio, A. Ruckenstein, Schumitt-Rink and C. Varma, Phys. Rev. B **43**, 10882 (1991).
25) W. Zheng and J. Oitmaa, cond-mat/0209305; cond-mat/0209307.
26) C. Jurecka and W. Brenig, Phys. Rev. B **64**, 092406 (2001).
27) F. F. Assaad, Phys. Rev. Lett. **83**, 796 (1999).
28) Z. P. Shi, R. R. P. Singh, M. P. Gelfand and Z. Wang, Phys. Rev. B **51**, 15630 (1995).
29) Z. Wang, X. P. Li and D. H. Lee, Physica (Amsterdam) **199B-200B**, 463 (1995).
30) Y. Matsushita, M. P. Gelfand and C. Ishii, J. Phys. Soc. Jpn. **66**, 3648 (1997).
31) S. Sachdev and N. Bhatt, Phys. Rev. B **41**, 9323 (1990).
32) S. Gopalan, T. M. Rice and M. Sigrist, Phys. Rev. B **49**, 8901 (1994).
33) Y. L. Lee, Y. W. Lee and C.-Y. Mou, Phys. Rev. B **60**, 13418 (1999).
34) C. Jurecka and W. Brenig, Phys. Rev. B **63**, 094409 (2001).
35) M. P. Gelfand and R. R. P. Singh, Adv. Phys. **49**, 93 (2000).
36) T. Sakai and M. Takahashi, J. Phys. Soc. Jpn. **58**, 3131 (1989).